Magnetic properties and phase diagrams of a bilayer spin-3/2 Ising model

L. Ayache, L. Bahmad*, A. Benyoussef and H. Ez-Zahraouy

,

Laboratoire de Magnétisme et Physique des Hautes Energies.
Département de Physique, Faculté des Sciences, B.P. 1014
Université Mohammed V, Rabat, Morocco

Abstract: The magnetic properties and phase diagrams of a bilayer spin-3/2 Ising model is studied, under the effect of crystal field, using the mean field (MF) theory and the Monte Carlo (MC) simulations. The ground state phase diagrams in the (J_{s1} / J, Δ_{s1} / J) and (J_{s2} / J, Δ_{s1} / J) planes are determined analytically. On the other hand, the magnetization and critical temperature are studied. The results found by the two methods are in good agreement with the ground state phase diagram. It was found that the critical temperature calculated by Monte Carlo simulations is less than that obtained by the mean field method, for both positive and negative crystal field acting on each layer of the film.

**Corresponding author: bahmad@fsr.ac.ma*

I. Introduction

Recently, magnetic thin films have gained increasing interest for nano and micro-machined system. Much effort has been devoted to investigate the criticality and other statistical properties of various Ising systems [1], [2] and [3], which would enable a deeper understanding of order-disorder phase transition. The spin−3/2 Ising model was introduced earlier [4] to explain phase transitions in $DyVO_4$. Since then the spin−3/2 Ising model was studied by many approximate techniques and it was found that its phase diagrams are much richer in comparison with the lower spin systems, i.e. spin−1/2 and 1. The study of magnetic thin films has received intense for both theoretical and experimental reasons. The phase transitions have been observed in a variety of systems including for example ^{4}He [5-6] and ethylene adsorbed on graphite [7-8]. The layering transitions in Ising thin films have been studied using a real space renormalization group [9] and transfer matrix method [10]. The Ising model has been investigated in detail using many approximate methods, namely, mean field approximation [11], Monte Carlo simulations [12-13], effective field method [14-16], constant coupling [17] and renormalization group [18] techniques. All of these approximate methods show the existence of a line of tricritical points [19] into a line of critical end point and one of double critical points [20-21]. On the other hand, various types of a phase diagrams of a spin−3/2 is studied in three-dimensional [22-23]. More recently, with the increased interest in thin films, many works have been devoted to the influence of the crystal field on the phase transitions of magnetic thin films [24-26]. Our aim in this work is to study, using mean-field theory (MF) and Monte Carlo (MC) simulations, the phase diagrams of a bilayer spin-3/2 Ising model. The paper is organized as follows. In Sec.2, we present the model, give the mean field equations of the different order parameters and brief description of the MC simulations. In Sec.3, we present the results found by mean-field theory and Monte-Carlo simulations, then we end in Sec.4, by a conclusion.

II. Model and methods

II.1. Model

The system we consider is the spin-3/2 Ising model of a simple-cubic lattice, infinite and symmetric in the x and y direction and finite thickness in the z direction, i.e., a film of N=2 ferromagnetic layer is shown in figure 1. The Hamiltonian of this system is given by:

$$H = -J_{s1}\sum_{i,j\in S_1} S_i S_j - J\sum_{i,j\in S_1,S_2} S_i S_j - J_{s2}\sum_{i,j\in S_2} S_i S_j - \Delta_{s1}\sum_{i\in S_1} S_i^2 - \Delta_{s2}\sum_{i\in S_2} S_i^2$$

where $S_i = \pm\frac{3}{2}, \pm\frac{1}{2}$; the first sum runs over all pairs of neighbors, $J\,(J=1)$ is the interlayer coupling constant between two surfaces, J_{s1} and J_{s2} are the coupling constants for neighbors of the first and the

 © 2010 The Moroccan Statistical Physical and Condensed Matter Society

second surfaces, respectively Δ_{s1} and Δ_{s2} are the crystal field of these surfaces.

Fig 1

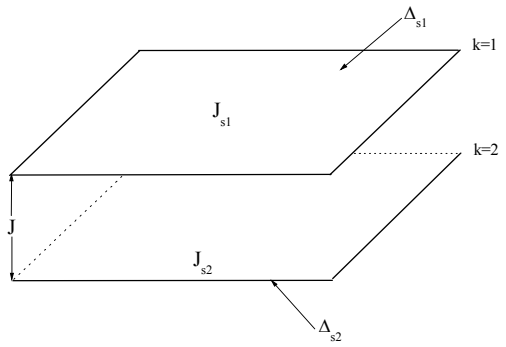

Figure 1: Geometry of thin film formed with two surfaces (k = 1, 2). The system is infinite in the x and y direction. J is the interlayer coupling constant between two surfaces, J_{s1} and J_{s2} are the coupling constants for neighbors of the first (k = 1) and the second surface (k = 2), respectively Δ_{s1}/J and Δ_{s2}/J are the crystal field of these surfaces.

II-2- Mean field theory

To write the mean-field equation let h_k denotes the molecular field associated with the order parameter m_k, expressed as:

$$h_1 = (zJ_{s1}m_1 + Jm_2)$$

$$h_2 = (zJ_{s2}m_2 + Jm_1)$$

The effective Hamiltonian of the system is:

$$\mathrm{H}_0 = -\sum_{i\in S_1} h_1 S_i - \sum_{i\in S_2} h_2 S_i - \Delta_{s1}\sum_{i\in S_1} S_i^2 - \Delta_{s2}\sum_{i\in S_2} S_i^2$$

it generates the following partition function:

$$Z_0 = Tr\ \exp -\beta \mathrm{H}_0 \qquad (3)$$

The magnetization of a surface k is given by:

$$m_k = < S_k > = \frac{Tr S_k \exp(-\beta \mathrm{H}_k)}{Tr \exp(-\beta \mathrm{H}_k)}$$

Where

$$\mathrm{H} = \sum_k \mathrm{H}_k = -\sum_k S_k h_k - \sum_k S_k^2 \Delta_{sk}$$

When expanding the Eq.(4), one can easily find the following expression [27-29]:

$$m_k = \frac{3\exp\frac{9\beta}{4}\Delta_{sk}\sinh\frac{3}{2}\beta h_k + \exp\frac{\beta}{4}\Delta_{sk}\sinh\frac{1}{2}\beta h_k}{2\exp\frac{9\beta}{4}\Delta_{sk}\cosh\frac{3}{2}\beta h_k + 2\exp\frac{\beta}{4}\Delta_{sk}\cosh\frac{1}{2}\beta h_k}$$

where $\beta = \frac{1}{k_B T}$ is the inverse temperature and k_B is the Boltzmann constant.

In these equations, m_k $(k = 1,2)$ is the reduced magnetization of the k[th] layer and z (z=4) is the interlayer coordination number. The total free energy of the film can be written as follows:

$$F = F_0 + < \mathrm{H} - \mathrm{H}_0 >_0$$

where

$$F_0 = -\frac{1}{\beta}\log Tr \exp -\beta \mathrm{H}_0$$

$$< \mathrm{H} - \mathrm{H}_0 >_0 = \frac{1}{2}(zJ_{s1}m_1^2 - 2Jm_1m_2 - zJ_{s2}m_2^2)$$

The total free energy of the film is given by:

$$F = -\frac{1}{\beta}\sum_{k=1}^{2}\ln\left[2\exp\frac{9\beta}{4}\Delta_{sk}\cosh\frac{3}{2}\beta h_k + 2\exp\frac{\beta}{4}\Delta_{sk}\cosh\frac{1}{2}\beta h_k\right] + \frac{1}{2}(zJ_{s1}m_1^2 - 2Jm_1m_2 - zJ_{s2}m_2^2)$$

II-3- Monte Carlo simulations

We have also performed Monte Carlo simulations to complement Mean field theory. A preliminary study showed that, when performing Monte Carlo simulations under the Metropolis algorithm [34] with periodic boundary conditions to update the lattice configurations, the relevant calculated quantities did not change appreciably when varying the number of spins of each plane from $N_x = N_y = 32$ to 128. Where N_x and N_y are the number of spins, of each plane, in the x and y-directions, respectively. Taking into account the above considerations, in all the following we will give numerical results for a $N_x = N_y = 64$ spins for each plane. The physical quantities of use are the magnetizations m_k; k = 1, 2 and are estimated by:

$$|m_k| = < |S_k| > \frac{1}{(N_x \times N_y)\times V}\sum_c\sum_i S_i$$

where i runs over the lattice sites and c runs over the configurations obtained to update the lattice over one sweep of the entire $N_x \times N_y$ spins of the lattice (one Monte Carlo step, MCS) counted after the system reaches thermal equilibrium and V is the number of the MCS.

In order to measure the phase boundaries we shall find useful the measurement of fluctuations in m_k defined by the magnetic susceptibility:

$$\chi_k = \frac{N_x \times N_y}{k_B T}(< m_k^2 > - < |m_k| >^2)$$

III-Results and discussions

III-1- Ground state

The ground state phase diagrams are calculated in order to determine the stable solutions of the model together with the free energy. Although the ground state phase diagrams can only help us at zero temperature, the zero temperature configurations are very important as a starting point in obtaining the temperature dependent phase diagrams. According to the study on the ground state, fired on two groups, the first one, is illustrated by figures (2a, 2b and 2c) in the $(J_{s1}/J, \Delta_{s1}/J)$ plane.

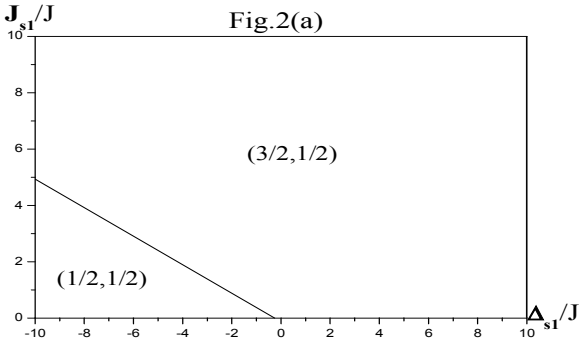

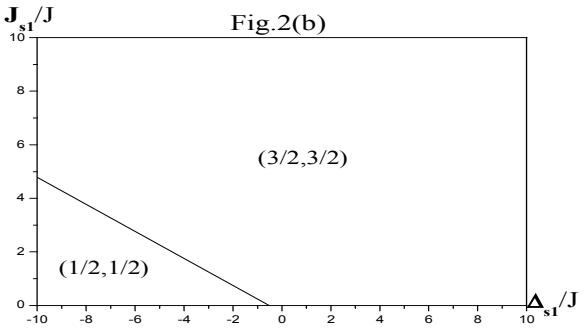

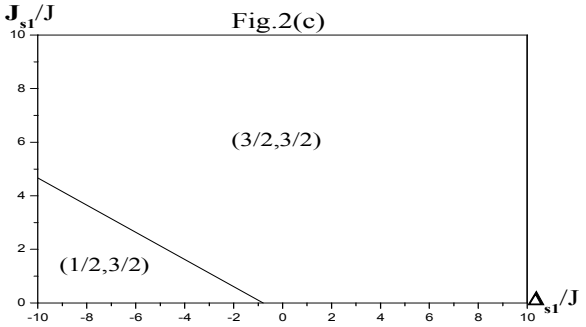

Figure 2: The ground-state phase diagrams in the $(J_{s1}/J, \Delta_{s1}/J)$ plane for different values of crystal field acting on the second surface (k = 2): (a) $\Delta_{s2}/J = -5$, (b) $\Delta_{s2}/J = -2.5$ and (c) $\Delta_{s2}/J = 5$, for $J_{s2}/J = 1 \cdot (3/2,3/2), (3/2,1/2), (1/2,3/2)$ and $(1/2,1/2)$ are the only stable phases for very low temperatures.

While the second one see figures (3a, 3b and 3c) shows the ground-state phase diagrams in the $(J_{s2}/J, \Delta_{s1}/J)$ plane.

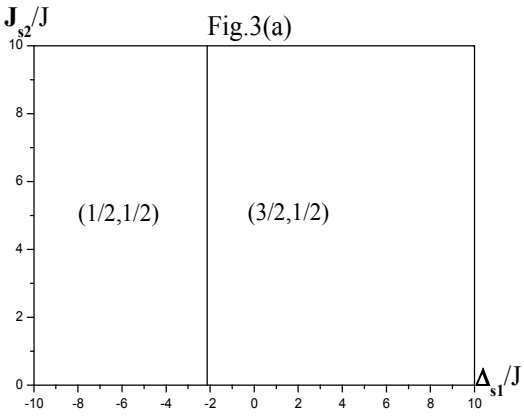

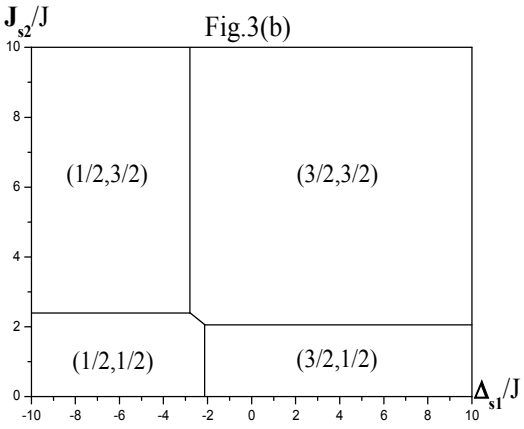

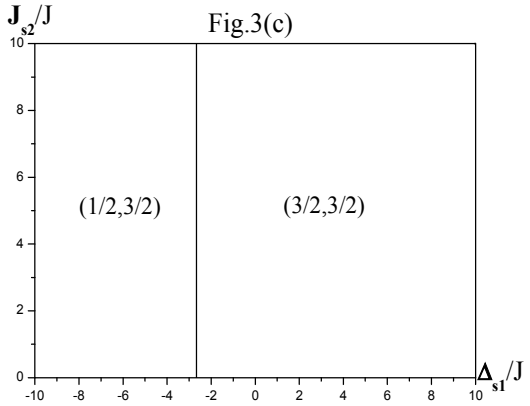

Figure 3: The ground-state phase diagrams in the $(J_{s2}/J, \Delta_{s1}/J)$ plane for different values of crystal field acting on the second surface (k = 2): (a) $\Delta_{s2}/J = -25$, (b) $\Delta_{s2}/J = -5$ and (c) $\Delta_{s2}/J = 5$, for $J_{s1}/J = 1$. $(3/2,3/2)$, $(3/2,1/2)$, $(1/2,3/2)$ and $(1/2,1/2)$ are the only stable phases for very low temperatures.

In the first family (see figures 2), we established the ground-state phase diagram in the $(J_{s1}/J, \Delta_{s1}/J)$ plane, for a fixed value of Δ_{s2}/J :(a) $\Delta_{s2}/J = -5$, (b) $\Delta_{s2}/J = -2.5$ and (c) $\Delta_{s2}/J = 5$. For example [see figure 2(a)] we distinguish two regions. (a) $J_{s1}/J < 4.93$, $\Delta_{s1}/J < -0.26$ and $J_{s1}/J + \Delta_{s1}/2J < -0.13$; the stable configuration is (1/2,1/2) where the spins of two layer are all equal to 1/2. (a) $J_{s1}/J > 0.26$, $\Delta_{s1}/J > 4.93$ and $J_{s1}/J + \Delta_{s1}/2J > -0.13$; the stable configuration is $(3/2,1/2)$ where the spins of the first layer are all equal to $3/2$ and of the second layer are all equal to $1/2$. From figure 2 the system has one transition by varying J_{s1}/J or Δ_{s1}/J. (a)(i) From the state $(1/2,1/2)$ to the state $(3/2,1/2)$ at $J_{s1}/J = -\Delta_{s1}/2J - 0.13$. (b)(i)From the state $(1/2,1/2)$ to the state $(3/2,3/2)$ at $J_{s1}/J = -\Delta_{s1}/2J - 0.26$. (c)(i) From the state $(1/2,3/2)$ to the state $(3/2,3/2)$ at $J_{s1}/J = -\Delta_{s1}/2J - 0.4$. In the second family (see figure 3), we established the ground-state phase diagram in the $(J_{s2}/J, \Delta_{s1}/J)$ plane, for a fixed value of Δ_{s2}/J :(a) $\Delta_{s2}/J = -25$,(b) $\Delta_{s2}/J = -5$ and (c) $\Delta_{s2}/J = 5$. For example [see Figure 3(b)] we distinguish four regions. (b) $J_{s2}/J < 2.4$, $\Delta_{s1}/J < -2.13$ and $J_{s2}/J + \Delta_{s1}/2J < 1$; the stable configuration is $(1/2,1/2)$ where the spins of two layer are all equal to 1/2. (b) $J_{s2}/J > 2.06$, $\Delta_{s1}/J > -2.8$ and $J_{s2}/J + \Delta_{s1}/2J > 1$; the stable configuration is (3/2,3/2) where the spins of two layer are all equal to 3/2. (b) $J_{s2}/J > 2.4$ and $\Delta_{s1}/J > -2.8$; the stable configuration is $(1/2,3/2)$ where the spins of the first layer are all equal to 1/2 and the second layer all equal to 3/2. (b) $J_{s2}/J < 2.06$ and $\Delta_{s1}/J > -2.13$ the stable configuration is $(3/2,1/2)$ where the spins of the first layer are all equal to 3/2 and the second layer all equal to 1/2. From figure 3(b) is clear that for fixed values of Δ_{s1}/J, the system exhibits various transitions by varying J_{s2}/J. For following ranges of variation of Δ_1/J : (b)(i) $-10 < \Delta_{s1} < -2.8$, (b)(ii) $-2.8 < \Delta_{s1} < -2.13$ and (b)(iii) $-2.13 < \Delta_{s1} < -10$, the system presents the following phase transitions. (b)(i) From the state $(1/2,3/2)$ to the state $(1/2,1/2)$ at $J_{s2}/J = 2.4$. (b)(ii) From the state $(3/2,3/2)$ to the state $(1/2,3/2)$ at $J_{s2}/J = -\Delta_{s1}/2J + 1$. (b)(iii) From the state $(3/2,3/2)$ to the state $(3/2,1/2)$ at $J_{s2}/J = 2.06$. From figure 3(a) and (c), the system has one transition by varying Δ_{s1}/J. (a)(i)From the state $(1/2,1/2)$ to the state $(3/2,1/2)$ at $\Delta_{s1}/J = -2.13$. (c) (i) From the state $(1/2,3/2)$ to the state $(3/2,3/2)$ at $\Delta_{s1}/J = -2.66$.

III-2- Phase diagrams at finite temperature

In this section, a detailed discussion dealing with finite temperature phase diagrams is discussed. Using mean field theory, the critical temperature is determined by solving numerically Eq. (6) which may have more than one solution; the one which minimizes the free energy [Eq. (10)] corresponds to the stable phase. However, the critical temperature of thin film as a function of the crystal field acting on the first surface, obtained from mean field theory, are shown, for $J_{s2}/J = 1$ and $\Delta_{s2}/J = -5$ in Fig. 4.

Fig. 4a

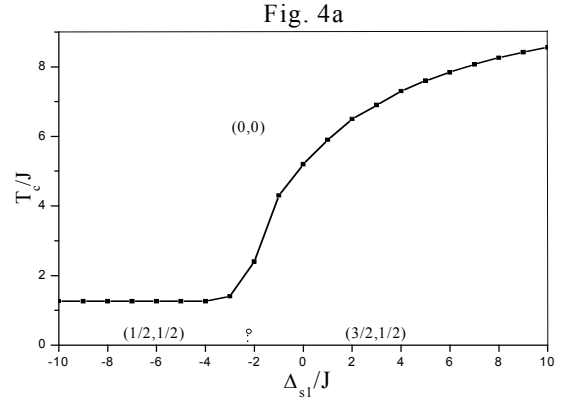

Fig. 4b

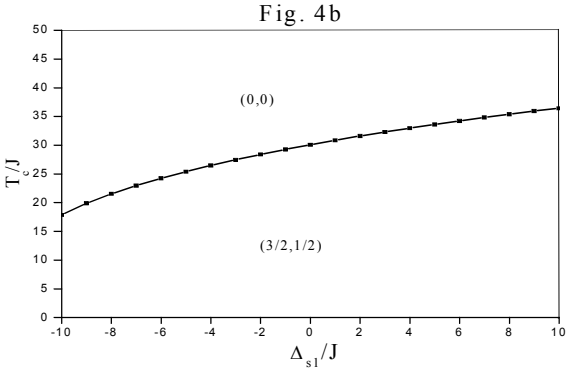

Figure 4: The critical temperature of the film as a function of Δ_{s1}/J, for $J_{s2}/J=1$ and $\Delta_{s2}/J=-5$, with two coupling constant values: (a) $J_{s1}/J=1$ and (b) $J_{s1}/J=6$, using Mean field theory.

acting on the first surface. For very low temperatures, we found a first-order transition line (dashed line) separating the phases $(1/2,1/2)$ and $(3/2,1/2)$. This first-order line is terminated by an isolated critical point located at $(\Delta_{s1}/J=-2.27, t=0.43)$. In Fig. 4b plotted for $J_{s1}/J=6$, the phase $(1/2,1/2)$ disappears at low temperature. Therefore, the second order transition-line temperature separates the ferromagnetic phase $(3/2,1/2)$ from the paramagnetic phase $(0,0)$ are greater than those found for $J_{s1}/J=6$. In order to complement the mean field theory, the critical temperature of thin film as a function of the crystal field acting on the first surface, obtained from Monte Carlo simulations, are shown, for $J=1$, $J_{s2}/J=1$ and $\Delta s2/J=-5$ in Fig. 5.

Fig. 5a

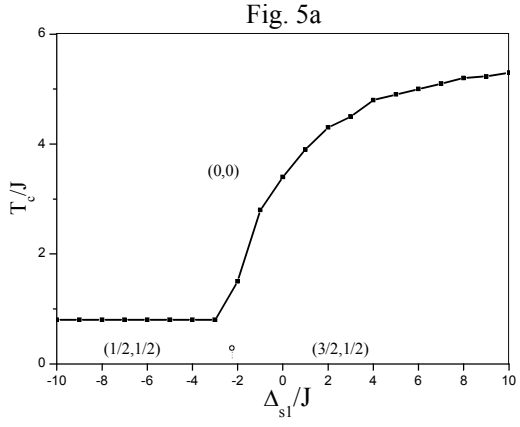

Fig. 5b

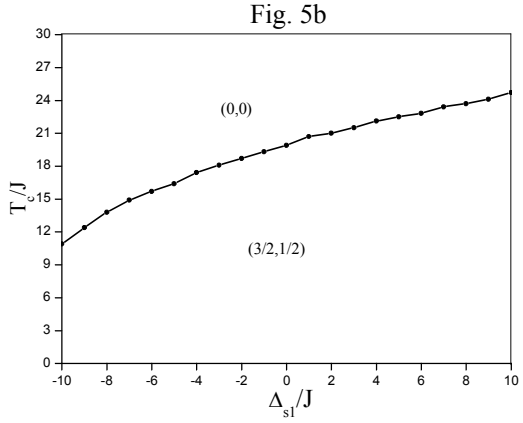

Figure 5: The critical temperature of the film as a function of Δ_{s1}/J, for $J_{s2}/J=1$ and $\Delta_{s2}/J=-5$, with two coupling constant values: (a) $J_{s1}/J=1$ and (b) $J_{s1}/J=6$, using Monte Carlo simulations.

The results found by Monte Carlo simulations, are similar to the MF one but the critical temperature are less than those of mean field theory. Thus, in Fig. 5a, for $J_{s1}/J=1$, we can show a first-order transition between $(1/2,1/2)$ and $(3/2,1/2)$ at $\Delta_{s1}/J=-2.25$. Indeed, for $J_{s1}/J=2$, Fig. 5b shows the existence of a second-order transition line between the paramagnetic $(0,0)$ and the partly ferromagnetic phase $(3/2,1/2)$.

In the two previous diagrams, we must separate two regions that depend on the sign of the crystal field acting on the first surface:

-In the first region, the crystal field acting on the first surface is negative, it promotes disorder.

-In the second region, the crystal field acting on the first surface is positive, it promotes the order.

It is important to mention from above results, the plateau disappears on in-creasing the crystal field and/or the coupling constants.

Using mean field theory, the critical temperature of thin film as a function of the crystal field acting on tow surfaces $(\Delta_{s1}/J=-\Delta_{s2}/J)$, is plotted for $J=1$, $(J_{s1}/J=J_{s2}/J=1)$ (Fig. 6).

Fig. 6

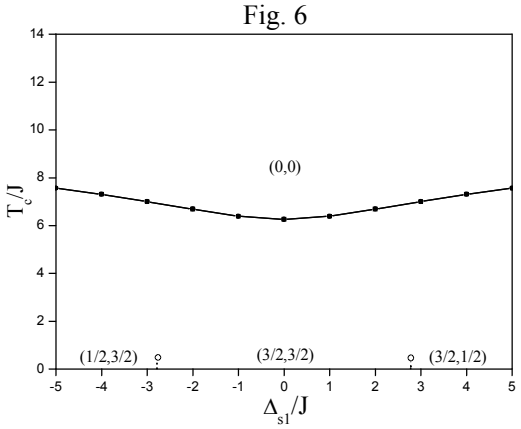

Figure 6: the critical temperature of the film a function of Δ_{s1}/J $(\Delta_{s2}/J=-\Delta_{s1}/J)$, for $J_{s1}/J=J_{s2}/J=1$, using Mean field theory.

In Fig. 6, the paramagnetic $(0,0)$ and ferromagnetic phases are separated by a second-order transition line (solid line). For very low temperatures, we found two first-order transition lines (dashed line). In one hand, a first-order transition line separating the phases $(1/2,3/2)$ and $(3/2,3/2)$, and terminated by an isolated critical point located at $(\Delta_{s1}/J=-2.78, t=0.3)$. On the other hand, a first-order transition line separating the phases $(3/2,3/2)$ and $(3/2,1/2)$, and terminated by an isolated critical point located at $(\Delta_{s1}/J=2.78, t=0.3)$.

In order to outline the effect of system behaviour as a function of the coupling
of the first surface J_{s1}/J we plot, in Figs. 7 and 8, the critical temperatures for several values of the crystal field $(\Delta_{s2}/J=-\Delta_{s1}/J)$. Indeed, for $\Delta_{s1}/J=5$, see Fig. 7, the second-order transition line separating the paramagnetic phase from the phase $(3/2,1/2)$. We remark that the behaviour of this line is linear. Whereas for $\Delta_{s1}/J=-5$, Fig. 8 shows the existence of a second-order transition line between the paramagnetic and the partly ferromagnetic phases and a first-order transition between the phases $(1/2,3/2)$ and $(3/2,3/2)$ terminated by an isolated critical point $(J_{s1}/J=2.11, t=0.35)$.

Fig. 7

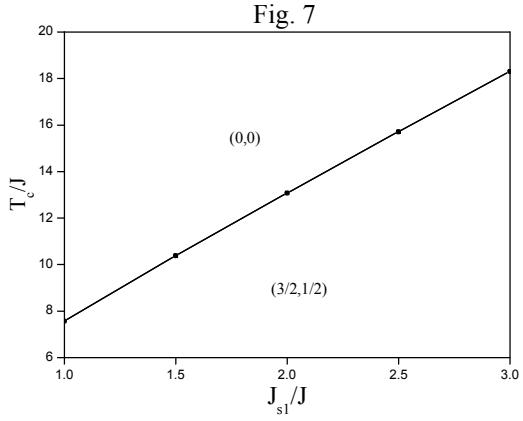

Figure 7: The critical temperature of the film as a function of J_{s1}/J, for $J_{s2}/J=1$ and $\Delta_{s1}/J=-\Delta_{s2}/J=5$.

Fig. 8

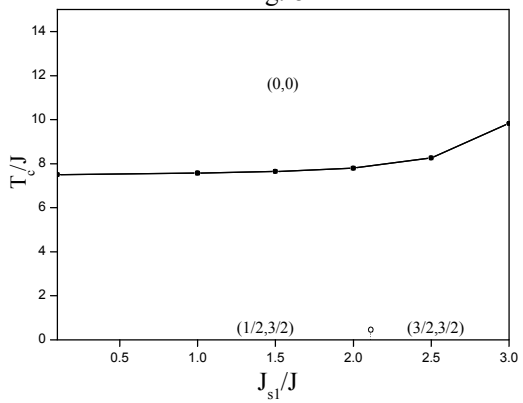

Figure 8: The critical temperature of the film as a function of J_{s1}/J, for $J_{s2}/J=1$ and $\Delta_{s1}/J=-\Delta_{s2}/J=5$.

III-3- Magnetic properties

In this part, we have studied the magnetization in order to complete the phase diagrams represented above. m_k is the magnetization of the kth surface. In Fig. 9, we plot the magnetization of two surfaces of the film as a function of the temperature, by mean field theory and Monte Carlo simulations, for $J_{s1}/J=J_{s2}/J=1$ and $\Delta_{s1}/J=-\Delta_{s2}/J=5$.

Fig. 9

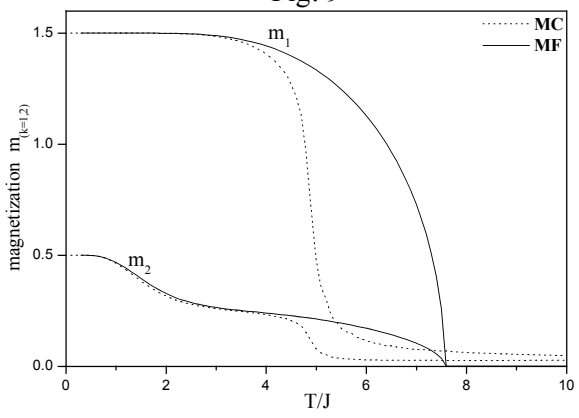

Figure 9: The magnetization of two surfaces (k = 1, 2) as a function of the temperature obtained within mean field theory and Monte Carlo simulations, for $J_{s1}/J = J_{s2}/J = 1$ and $\Delta_{s1}/J = -\Delta_{s2}/J = 5$.

The increasing temperature effect is to decrease this magnetization. As seen $m_1 = 1.5$ and $m_2 = 0.5$. Moreover, the all surfaces disorder near the critical temperature $Tc_{MF} = 7.5$, in the case of mean field theory, and $Tc_{MC} = 4.9$ for the Monte Carlo simulations. It is worth noting that for very low temperature, MF and MC are in good agreement with the ground state phase diagram. The magnetization m_k of each surfaces (k=1,2) are depicted in Fig.10 for $\Delta_{s1}/J = -\Delta_{s2}/J = 3$ and $J_{s1}/J = J_{s2}/J = 1$.

Fig. 10

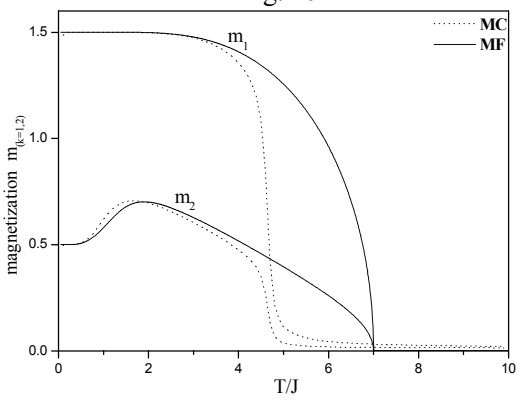

Figure 10: The magnetization of two surfaces (k = 1, 2) as a function of the temperature obtained within mean field theory and Monte Carlo simulations, for $J_{s1}/J = J_{s2}/J = 1$ and $\Delta_{s1}/J = -\Delta_{s2}/J = 3$.

Furthermore, it is found that the magnetization of each surfaces, decrease with increasing the temperature, except for the second surface k = 2, exhibits a short increasing at low temperature. This phenomenon is be explained by the competition between the crystal field acting on the surfaces and the order-disorder.

In Fig. 11, we plot the magnetization of the first surface m1 for different values of J_{s1}/J by two methods MF theory and MC simulations. The starting values of m_1 at low temperature are in concordance with those obtained in ground state phase diagram.

Fig. 11

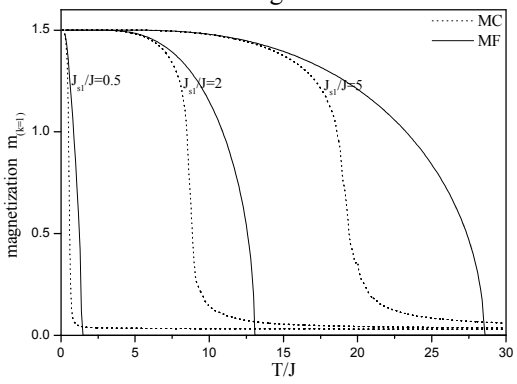

Figure 11: The magnetization of the first surface (k = 1), as a function of the temperature obtained within Monte Carlo simulations, for $J_{s2}/J = 1$ and $\Delta_{s1}/J = -\Delta_{s2}/J = 5$ with different values of J_{s1}/J : 0.5, 2 and 5.

The results found by two methods are qualitatively identical, since the critical temperature for first surface increase with increasing the J_{s1}/J.

Finally we show in Fig. 12 the magnetization of the first surface m_1 as a function of temperature obtained by mean field theory and Monte Carlo simulation, for $J_{s1}/J = J_{s2}/J = 1$ and $\Delta_{s1}/J = -\Delta_{s2}/J = 5$.

The increasing temperature effect is to decrease these magnetization amplitudes plotted in Fig. 12 by two methods. Numerical value computed by MC method (Tc_{MC}/J) are found to smaller than those obtained using MF theory (Tc_{MF}/J).

Fig. 12

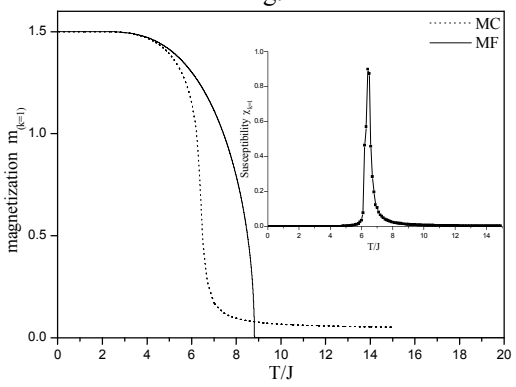

Figure 12: The magnetization of the first surface (k = 1), as a function of the temperature obtained within mean field theory and Monte Carlo simulations, for $J_{s1}/J = J_{s2}/J = 1$ and $\Delta_{s1}/J = \Delta_{s2}/J = 5$.

However, the results predicted by two methods become similar, and are exactly those given by the ground state phase diagram, for very low temperature. In addition to magnetization, in the inset, the second order phase transitions have been determined by the magnetic susceptibility.

IV-Conclusions

Using Monte Carlo (MC) simulations and the mean field theory (MF), we have studied a bilayer spin-3/2 Ising model under the influence of a crystal field. The two methods are in agreement with the ground state phase diagrams, i.e. they converge to the same state value when the temperature tends to zero. The results obtained by the means-field theory are higher than those predicted by MC, since they have a certain uncertainty decreases with increasing the size unlike the case of the means field. Both methods provide critical properties of the system.

V. References

[1] T. Kaneyoshi, J. Mielnicki, T. Balcerzak and G. Wiatrowski Phys. Rev. B **42**, 4388 (1990).
[2] S. Grollau, Phys. Rev. E **65**, 056130 (2002).
[3] A. Bobak, F.O. Abubrig and T. Balcerzak, Phys. Rev. B **68**, 224405 (2003).
[4] J. Sivardire and M. Blume, Phys. Rev. B **5**, 1126 (1972).
[5] S. Ramesh and J. D. Maynard, Phys. Rev. Lett. **49**, 47 (1982).
[6] S. Ramesh, Q. Zhang, G. Torso and J. D. Maynard, Phys. Rev. Lett. **52**, 2375 (1984).
[7] M. Sutton, S. G. J. Mochrie and R. J. Birgeneau, Phys. Rev. Lett. **51**, 407 (1983); S. G. J. Mochrie, M. Sutton, R. J. Birgeneau, D. E. Moncton and
P. M. Horn, Phys. Rev. **30**, 263 (1984).
[8] S. K. Stija, L. Passel, J. Eckart, W. Ellenson and H. Patterson, Phys. Rev.
Lett. **51**, 411 (1983).
[9] A. Benyoussef and H.Ez-Zahraouy, Physica A **206**, 196 (1994)
[10] A. Benyoussef and H. Ez-Zahraouy, J. Phys. I. France **4**, 393 (1994)
[11] M. Keskin, O. Canko and M. Kirak, J. Stat. Phys. **127**, 359 (2007).
[12] Akai Kurbanovich Murtazaeva, b and Albert Babaevich Babaeva, J. Magn.
Magn. Mat. **321**, 2630 (2009).
[13] P. Cossio, J. Mazo-Zuluagaa and J. Restrepo, Phys. B **384**, 226 (2006).
[14] M. Kerouad, A. El-Atri, A. Ainane and M. Saber, Phys. Stat. Sol. (b) **195**,
519 (2006).
[15] Ya-Qiu Liang, Guo-Zhu and WeiQi Zhang, J. Magn. Magn. Mat. **265**, 305 (2003).
[16] M. Jaur, T. Kaneyoshi, Phys. A **195**, 497 (1993)
[17] P. W. Kasteleijn, Physica A **22**, 387 (1956).
[18] W. J. Song and C. Z. Yanc, Phys. Stat. Sol. (b) **186**, 511 (1994).
[19] H. Ez-Zahraouy and A. Kassou-Ou-Ali, Phys. Rev. B **69**, 064415 (2004).
[20] J. A. Plascak and D. P. Landau, Phys. Rev. E **67**, 015103 (2003).
[21] Y. L. Wang and K. Rauchwarger, Phys. Lett. A **59**, 73 (1976)
[22] T. Horiguchi, A. Lipowski and N. Tsushima, Phys. A **224**, 226 (1996).
[23] O. Canko and M. Keskin, Phys. Lett. **320**, 22 (2003).
[24] T. Balcerzak, J. Magn. Magn. Mat. **137**, 57 (1994).
[25] L. Bahmad, A. Benyoussef and H. Ez-Zahraouy, J. Magn. Magn. Mat. **251**, 115 (2002).
[26] Wei Jiang, Guo-Zhu Wei and Zi-Huo Xin, J. Magn. Magn. Mat. **217**, 225 (2000).
[27] A. Coniglio, F. di Liberto, G. Monroy, and F. Peruggi, Phys. Rev. B **44**, 12605 (1991).
[28] Grgory Geneste, Phys. Rev. B **79**, 144104 (2009)
[29] M.P. Kozlovskiia, I.V. Pylyuka and O.O. Prytula, Nuclear Physics B **753**, 242 (2006).